

Mixed Convection and Heat Transfer in a “T” Form Cavity: The Effect of Inclination

M'barka Mourabit¹, Hicham Rouijaa¹, El Alami Semma¹, Mustapha El Alami² and Mostafa Najam²

Abstract: We study the effect of inclination angle on mixed convection in a “T” form cavity containing two openings and two heated blocks mounted on its lower wall. The blocks are maintained at a constant temperature T_H . The lower wall is adiabatic and submitted to a vertical air jet while the upper wall is kept cold at a constant temperature $T_C < T_H$. The vertical walls are rigid and adiabatic. The governing equations are solved by a finite volume method. Special attention is devoted to the solution symmetry, the flow structure and the heat exchange through the cavity. The considered control parameters are: the inclination angle $0^\circ \leq \varphi \leq 90^\circ$, the Rayleigh number $10^5 \leq Ra \leq 10^6$, the Reynolds number $100 \leq Re \leq 1000$, the Prandtl number $Pr=0.72$, the height of the blocks $B=0.5$, the opening width $C=0.15$ and the distance between blocks $D=0.5$. The results are presented in terms of streamlines, isothermal lines and variations of Nusselt number with Re or φ .

Nomenclature

A	aspect ratio of calculation domain ($A = L'/H'$)
B	dimensionless block height ($B = h'/H'$).
C	dimensionless openings diameter ($C = l'/H'$)
D	dimensionless space between blocks ($D = d'/H'$)
d'	space between adjacent blocks (m)
H'	cavity height (m)
h'	blocks height, (m)
L'	horizontal length of calculation domain (m)
l'	opening diameter (m)
g	acceleration due to gravity (m/s^2)

¹ Laboratoire de Mécanique, Faculté des Sciences et Techniques, Université Hassan Ier, BP. 577 Settat, Maroc.

² Laboratoire LPMMAT, Département de Physique, Faculté des Sciences Aïn Chock, Université Hassan II Casablanca. BP. 5366 Maarif, Casablanca, Maroc.

Nu_g	mean Nusselt number
Nu_L	local Nusselt number along the planes of the left block
Nu_R	local Nusselt number along the planes of the right block
Pr	Prandtl number ($Pr = \nu/\alpha$)
Re	Reynolds number ($Re = U_0 \times H'/\nu$)
θ	dimensionless temperature, $(T - T_C)/(T_H - T_C)$
T	temperature of the fluid
ΔT	temperature difference ($T_H - T_C$)
Ra	Rayleigh number, ($Ra = g\beta\Delta T'H'^3/(\alpha\nu)$)
U_0	Characteristic velocity of the forced flow
x, y	dimensionless Cartesian coordinates in the two directions $(x, y) = (x', y')/H'$
(u, v)	velocities.
(U, V)	dimensionless velocities $(U, V) = (u, v)/U_0$

Greek letters

α	thermal diffusivity (m^2s^{-1})
β	volumetric coefficient of thermal expansion (K^{-1})
φ	inclination angle of the cavity
λ	thermal conductivity ($Wm^{-1}K^{-1}$)
ν	cinematic viscosity (m^2s^{-1})
ρ	fluid density (kg/m^3)
ψ	dimensionless stream function, $\psi = \psi'/\alpha$
Ω	dimensionless vorticity $\Omega = \Omega' H'^2/\alpha$

Subscripts

H	Heated wall
C	Cold wall

1 Introduction

Many investigations, about heat transfer in a channel containing blocks, have been conducted these two last decades. Because of, its application in various domains such as: electronics industry. Where, over heat issues is one of electronic components drawbacks, resulting from their feature sizes decreasing and package densities increasing [Bejan et al. (1992); Chen et al. (2004), Sharma et al. (2012)]. The excess heat generated in the electronic devices must be dissipated for preventing

its damage. For that, a number of studies have been proposed in the literature in order to remove heat from integrated circuits. Initially, a numerical study of forced convective cooling of an array of obstacles was performed by Zeng et al. (2009) to synthesize the effects of various pertinent parameters on the cooling performance. Several pertinent physical attributes for this array of obstacles were discussed. In addition, Young et al. (1998) have presented two numerical studies of the fluid and thermal transport within a two-dimensional channel containing heated obstacles. These investigations detail the effects of variations in the obstacle height, width, spacing, and number, along with the obstacle thermal conductivity, fluid flow rate, and heating method, to illustrate important fundamental and practical results. Nevertheless, Amahmid et al. (1997) studied numerically the fluid flow and heat transfer induced by natural convection in a finite horizontal channel containing an indefinite number of uniformly spaced rectangular blocks on its lower wall. The influence of Rayleigh number, the computation domain on the flow structure and heat transfer in stationnar regime. The effect of the computation domain choice on the multiplicity of the solution was studied. The effect of each solution on the flow and the heat transfer was examined. However, Najam et al. (2004) has studied numerically the enhancement of heat transfer in a cavity with heated rectangular blocks and submitted to a vertical jet of fresh air from below. For a given Re , the study shows that there exist multiple solutions of the problem on which the resulting Nusselt number depends significantly. Most, mixed convection in a horizontal channel containing heated blocks on its lower wall was studied numerically by Najam et al. (2003). It was demonstrated that there exists a critical Re above which the natural convection cells are carried down stream by the forced flow. The displacement of the cells can be observed even in situations where the flow is dominated by natural convection. Bakkas et al. (2006) have studied numerically two dimensional, steady, laminar natural convection in a horizontal channel provided with heating blocks. The effect of the computation domain on the multiplicity of solutions was studied. It was found that a solution obtained in the case of a simple domain could be unstable in the double domain, and this depended on the governing parameters. They observed different flow patterns in the channel while varying the governing parameters. Moreover, El Alami et al. (2004) have studied the chimney effect and natural convection heat transfer in a “T” shaped cavity. The results show that the blocks height has an important effect on the mass flow rate and average Nusselt number. M and Nu increase with B . For relatively high values of Ra ($Ra \geq 3 \times 10^5$), the height effect on the mass flow rate becomes negligible. El Alami et al. (2009) have conducted a numerical investigation to evaluate heat transfer and mass flow rate induced by natural convection in a finite channel with heated rectangular blocks at the bottom. The results show the existence of different solutions of the problem (ICF, ECF and MS) on which the resulting heat transfer and mass flow

rate depend significantly. While, Meskini et al. (2011) have investigated mixed convection in a square cavity containing rectangular heated blocks (an inverted “T” shaped cavity) on its upper wall. The results show three solutions when varying Re and Ra: ECF, ICF and FF. It was demonstrated that there is a critical Re (Re_{cr}) above which the natural convection cells disappear and the flow in the cavity is governed by forced convection (FF solution). Non symmetric solutions have been at low Re, for all choose values of B, while the boundary conditions and the geometry of the system are symmetric. Re_{cr} increases with Ra for each value of B. Nu increases with Re and B. Rouijaa et al. (2011) have studied numerically the enhancement of heat transfer in an inclined cavity with heated rectangular blocks. The results show the existence of different solutions, in the range of $0 \leq \varphi \leq 90^\circ$, on which the resulting heat transfer and mass flow rate depend significantly.

Recently, many relevant works have been conducted on heat transfer in enclosures of different shapes, such as conjugate heat transfer, across a vertical solid wall separating natural convection in a cold fluid-saturated porous medium and film condensation in a saturated-vapor medium, which was analyzed by Al-Ajmi et al. (2011). Arid (2012) et al. have developed a two-dimensional numerical model in order to investigate the phase-change of ice near 4°C in a rectangular cavity. Results confirm the possibility to control the typical dynamics of ice melting in a square cavity near the density inversion point by means of a wall temperature which varies in time (with given amplitude and frequency).

The focus on natural convection has been done in different studies like [Lappa et al. (2011-2013); Dihmani et al. (2012); Hamimid et al (2012)]. Most, Mahmoudi et al. (2013) have also solved the steady-state laminar natural convective heat-transfer problem in a triangular cavity filled with air ($Pr=0.71$) by using a double-population Lattice Boltzmann Method (LBM). It was observed that inclination angle can be used as a relevant parameter to control heat transfer in right-angled triangular enclosures. More, the effect of the hydraulic heterogeneity on natural convection in a rectangular cavity has been investigated by Choukairy et al. (2012). Experimental and numerical observations of oscillatory instability of melt flow in a Czochralski model were compared, and a disagreement observed at small crystal dummy rotation rates was addressed Haslavsky et al. (2013). Hydrodynamic and heat transfer experiments have been conducted in a vertical channel filled with metal foams of different foam thicknesses. The results of the hydrodynamic experiments show that the variation of pressure drop with the foam thickness is insignificant Kamath et al. (2013). The results of the hydrodynamic experiments show that the variation of pressure drop with the foam thickness is insignificant. However, an increase in the foam thickness results in an increase in the heat transfer compared to an empty channel of same channel width and Re_H . The attendant increase in pumping power

for a heat transfer enhancement of 350 W, over an empty channel is found to be only 9 W.

Maougat et. al (2013) have studied numerically the irreversibility and heat transfer properties of a steady laminar mixed flow in a square cavity, filled with a saturated porous medium and heated by a discrete set of heat sources. The heat transfer is improved by increasing the Reynolds and Prandtl numbers. They have the same effect on the entropy production. It is interesting to note that it has a profitable effect when the porous medium is introduced into the cavity in the sense where a better heat transfer and lowest entropy production are obtained. This is in agreement with EGM principle. Entropy generation rate, Bejan number and heat transfer increases with Da . Re and Pr have the same effect on the Bejan number and the entropy generation rate increases with the irreversibility distribution ratio. There is an aspect ratio for which the entropy generation and heat transfer are maximum, it can be concluded that the physical system must be stable for this value and the EGM principle is not applicable for this case.

Mahrouche et al. (2013) have investigated numerically mixed convection in a rectangular partitioned cavity equipped with two heated partitions at a constant temperature, T_C . The results show that the flow and heat transfer depend significantly on Reynolds number, Re , and block height, B . In addition, Moufekkik et al. (2012) have examined numerically the problem related to coupled double diffusive convection in a square enclosure filled with a gray gas in the presence of volumetric radiation. Results show that for the case of cooperating flows, the isotherms and isoconcentrations are inclined in the core cavity and the flow is relatively stable whereas multicellular recirculations appear in the opposing-flows case. Generally when the mass effect is dominant, the flow is slowed and the influence of radiation is considerable on the thermal field and negligible on the dynamic and concentration fields. However, when thermal effects are dominant, the volumetric radiation accelerates the flow and significantly alters the structure of velocity, concentration and temperature fields. Rana et al. (2012) have investigated the effect of suspended particles on thermal convection in Rivlin-Ericksen elasticoviscous fluid heated from below in a Brinkman porous medium. It was observed that the medium permeability, suspended particles, gravity field and viscoelasticity introduce oscillatory modes. For stationary convection, it was observed that the Darcy number has stabilizing effect whereas the suspended particles and medium permeability had destabilizing effects on the system. The effects of suspended particles, Darcy number and medium permeability has also been shown graphically to depict the stability characteristics which are in good agreement with the results derived analytically.

Most of the previous studies were considered in natural or mixed convection in en-

closures or “T” shaped cavities without inclination. The present investigation studies numerically the effect of inclination angle on mixed convection in a “T” form cavity. Where, the mixed convection in an inclined “T” form cavity was the object of limited number of works. For that the aim of this work is in studying numerically the effect of inclination angle on mixed convection in a “T” form cavity with heated blocks on its lower wall and two openings formed on the horizontal walls. The upper wall is insulated. The vertical walls and the lower wall are adiabatic. A fresh air jet is sent through the inlet opening in order to promote an important heat exchange between the vertical planes of the blocks and the fluid flow. We will examine the influence of inclination angle on the solution symmetry, the multiplicity of solutions (if exists), the flow structure and the heat transfer.

2 Physical problem and governing equations:

Fig.1 shows a schematic representation of the problem. We consider a “T” form cavity containing two openings and two heated blocks mounted on its lower wall and maintained to a constant hot temperature T_H . The upper wall is cold at $T_C < T_H$. The vertical walls and the lower wall are adiabatic. The height of the blocks is constant $B=0.5$.

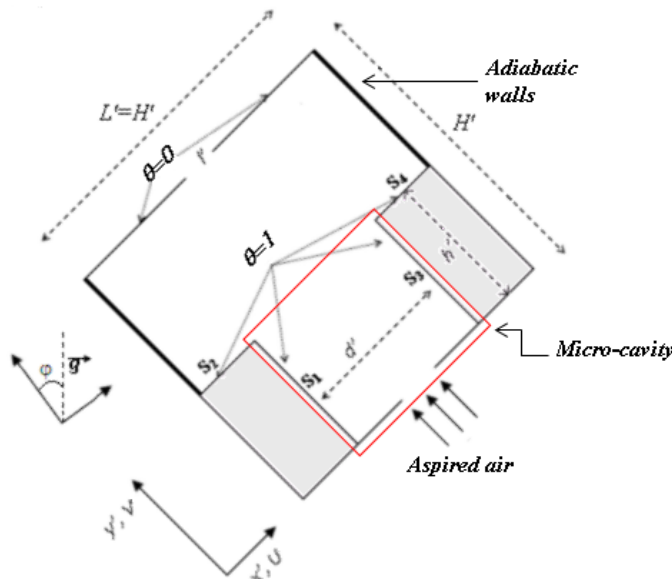


Figure 1: Schematic representation of the problem.

2.1 Governing equations:

The fluid is supposed bidimensionnal, laminar and incompressible. The fluid properties are constant and the Boussineq approximation is validated.

The dimensionless governing equations in term of temperature θ , velocities U and V are:

$$\frac{\partial U}{\partial x} + \frac{\partial V}{\partial y} = 0 \tag{1}$$

$$\frac{\partial U}{\partial t} + U \frac{\partial U}{\partial x} + V \frac{\partial U}{\partial y} = -\frac{\partial P}{\partial x} + \frac{1}{Re} \left(\frac{\partial^2 U}{\partial x^2} + \frac{\partial^2 U}{\partial y^2} \right) + \left(\frac{Gr}{Re^2} \theta \right) \sin \varphi \tag{2}$$

$$\frac{\partial V}{\partial t} + U \frac{\partial V}{\partial x} + V \frac{\partial V}{\partial y} = -\frac{\partial P}{\partial y} + \frac{1}{Re} \left(\frac{\partial^2 V}{\partial x^2} + \frac{\partial^2 V}{\partial y^2} \right) + \left(\frac{Gr}{Re^2} \theta \right) \cos \varphi \tag{3}$$

$$\frac{\partial \theta}{\partial t} + U \frac{\partial \theta}{\partial x} + V \frac{\partial \theta}{\partial y} = \frac{1}{Re Pr} \left(\frac{\partial^2 \theta}{\partial x^2} + \frac{\partial^2 \theta}{\partial y^2} \right) \tag{4}$$

The dimensionless governing equations for mass, momentum and energy conservation can be written as follows:

$$\frac{\partial \varphi}{\partial t} + \frac{\partial(U\varphi)}{\partial x} + \frac{\partial(V\varphi)}{\partial y} = \Gamma \nabla^2 \varphi + S_\varphi \tag{5}$$

We find the problem equations [1-4] by replacing φ , Γ and S_φ by the corresponding terms:

	φ	Γ	S_φ
Mass equation	1	0	0
Momentum equation	(U, V)	$\frac{1}{Re}$	$-\frac{\partial P}{\partial x_i} + \frac{Gr}{Re^2} \theta \delta_{i,2}$
Energy equation	θ	$\frac{1}{Re Pr}$	0

With: Pr is Prandtl number, Ra is Rayleigh number and Gr is Grashoff number. They are given by:

$$Pr = \frac{\nu}{\alpha}; \quad Ra = \frac{g\beta\Delta TH^3}{\nu\alpha}; \quad Gr = Ra Pr$$

The mean Nusselt number over the active walls is:

$$Nu_g = \int_0^B \frac{\partial \theta}{\partial x} \Big|_{x=0.25} dy + \int_0^{0.25} \frac{\partial \theta}{\partial y} \Big|_{y=B} dx + \int_0^B \frac{\partial \theta}{\partial x} \Big|_{x=0.75} dy + \int_{0.75}^1 \frac{\partial \theta}{\partial x} \Big|_{y=B} dx \tag{6}$$

The global Nusselt number on the left blocks planes is:

$$Nu_L = \int_0^B \frac{\partial \theta}{\partial x} \Big|_{x=0.25} dy + \int_0^{0.25} \frac{\partial \theta}{\partial y} \Big|_{y=B} dx \tag{7}$$

The global Nusselt number on the right blocks planes is:

$$Nu_R = \int_0^B \frac{\partial \theta}{\partial x} \Big|_{x=0.75} dy + \int_{0.75}^1 \frac{\partial \theta}{\partial y} \Big|_{y=B} dx \tag{8}$$

The dynamic and thermal boundary conditions associated to the problem equations (1-4) are:

- $y=0; 0.425 \leq x \leq 0.575$ (admission opening) $\theta = U = 0, V = 1$
- $y=0; 0.25 \leq x \leq 0.425$ and $0.575 \leq x \leq 0.75$ (The parts of lower wall separating the opening and the blocks) $U = V = 0, \frac{\partial \theta}{\partial y} = 0$
- $B \leq y \leq 1; x=0$ and $x=1$ (adiabatic vertical walls) $U = V = \frac{\partial \theta}{\partial x} = 0$

$U = V = 0$ On the rigid walls

The θ, U and V values in the evacuation opening are extrapolated by imposing the second derivatives null with respect to y , El Alami et al. (2005).

2.2 Numerical method:

The governing equations are solved by the finite volume method and SIMPLEC algorithm for the treatment of Velocity-Pressure coupling is used Patankar et al. (1980). The quadratic differentiation scheme: Quick has been adapted to the discretization of all convective terms of the transport equation Leonart et al. (1979). The mesh size is 80x80. The time step considered in this study is between 10^{-4} and 10^{-3} . The code is validated by comparing our results with those obtained by Kalache (1987) in case of natural convection flows inside trapezoidal cavity, then with results obtained in natural convection in a vertical channel by Desrayaud and Fichera (2002). This comparison gives a good agreement.

The finite volume governing equations for a general variable ϕ_P are given as follow:

$$A_P \phi_P = A_E \phi_E + A_W \phi_W + A_N \phi_N + A_S \phi_S + B$$

Where P, W, E, N, S denote cell location, west face of the control volume, east face of the control volume, north face of the control volume and south face of the control volume respectively and B is a constant.

3 Results and discussion:

The results will be presented in terms of flow structure, isothermal lines and heat transfer (Nusselt number) for ranges of inclination angle between 0° and 90° , Reynolds number between 100 and 1000 and $10^5 \leq Ra \leq 10^6$.

3.1 Flow structure and isothermal lines:

When varying ϕ , Re and Ra, we notice two different solutions ICF (*Intra Cellular Flow*), which was obtained by El Alami (2005) and UCLF (*Uni Cellular Left Flow*) was obtained by Najam and al (2003). The solution ICF is symmetric with respect to the vertical axis passing through the middle of the two openings, where its flow structure is composed of two Rayleigh-Bénard cells, recirculation cells and opening lines. However, the flow structure of the solution UCLF, generally, is composed of one convective cell above the left block, recirculation cells and open lines. More, we note that the flow structure of these solutions depend on the conflict between natural and forced convection when varying Re and ϕ . The forced flow is installed when Ra increases. We will present three cases: $Ra=10^5$, $Ra=5 \times 10^5$ and $Ra=10^6$.

a. Case of $Ra=10^5$

In this section, the flow structure is symmetric for all cases without inclination ($\phi = 0^\circ$). Where at $Re=100$, *Fig.2a*, obtained by Najam and al (2003), we notice that the solution ICF is symmetric. The flow structure is constituted of two convective cells: one above each block, two recirculation cells and open lines which pass between the convective cells. The isothermal lines display that the micro-cavity is filled by the fresh air. The isotherms are very tight near the block planes which imply a good ventilation of all these planes (S_1 , S_2 , S_3 and S_4). By increasing Re to 300, $\phi = 0^\circ$, we note that the convective cells disappear and two recirculation cells appear because the forced flow dominates on the natural convection as illustrated in *Fig.2b*. This figure illustrates also, that the vertical planes of the blocks are well ventilated while the absence of the convective cells leads to a bad ventilation of the horizontal planes. However, at $Re=500$, $\phi = 0^\circ$, we note that the Rayleigh-Bénard cells appear again, they are pushed by the air jet to the adiabatic vertical walls as shown in *Fig.2c*, in addition, the recirculation cells size increases. The tightness of the isotherms shows a well ventilation of the planes S_1 , S_2 , S_3 and S_4 . Besides, there is no good heat exchange between the vertical walls of the cavity and the air jet. The air jet arrives to the top of the cavity. By increasing Re to 1000, $\phi = 0^\circ$, *Fig.2d*, we notice that the solution is still symmetric (ICF). The recirculation cells lie and mix with those of Rayleigh-Bénard. The open lines are intensive and parallel to the symmetry axis. The corresponding isothermal lines show that all the

block planes are well ventilated, especially, the horizontal ones which is due to the rotation of the convective cells. They show also, that there is a bad heat exchange for the vertical walls of the cavity.

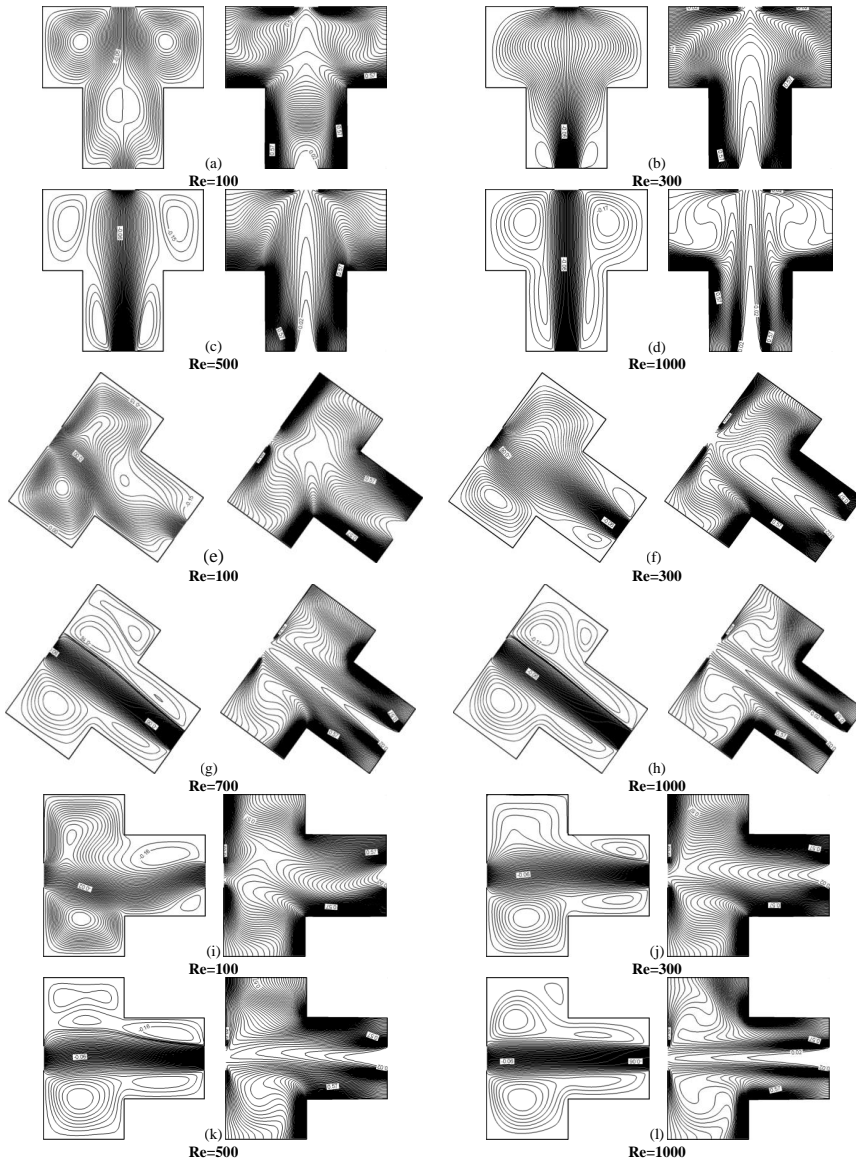


Figure 2: Streamlines and isotherms for $Ra=10^5$ and for different values of φ ; $\varphi=0^\circ$: {(a),(b),(c),(d)}; $\varphi=54^\circ$: {(e),(f),(g),(h)}; $\varphi=90^\circ$: {(i),(j),(k),(l)}

When we incline the cavity, we remark that the inclination has destroyed the symmetry of the solution as shown in *Fig.2e,f,g,h* for $\varphi = 54^\circ$. At $Re=100$, we obtain the UCLF solution which is already obtained by Najam and al (2003). According to *Fig.2e*, the flow structure is composed of one convective cell above the left block, recirculation cells and open lines that flow mostly near the left vertical planes. The corresponding thermal fields display an important cooling of the left block and a part of the plane S_3 . The air flow fills the micro-cavity and arrives at the upper part of the cavity. At $Re=300$, $\varphi = 54^\circ$, *Fig.2f*, we remark the same phenomenon as the previous case, with the intensification of the left recirculation cell size. More, all the planes are well ventilated except the right part of the plane S_4 because; there is no convective cell above this plane. For, $Re=700$, $\varphi = 54^\circ$, the convective cell size is decreased by the forced flow effect as displayed in *Fig.2g*. Moreover, the recirculation cells sizes increase, where the right cell lies and mixes with the convective one. The isotherms of this case display that the inferior parts of the heated planes S_1 and S_3 are not well ventilated. Otherwise, we show that there is no good heat exchange through the horizontal plane S_4 . However, the increase of Reynolds number up to 1000, $\varphi = 54^\circ$, helps the solution to recover its symmetry as shown in *Fig.2h*. Most this figure shows the existence of two convective cells which are mixed with those of recirculation and a small cell above the right block. The isothermal lines illustrate the same phenomenon as the previous case ($Re=700$).

By increasing the inclination angle $\varphi = 90^\circ$ and $Re=100$ *Fig.2i*, we obtain also, UCLF solution. The flow structure is made up of a convective cell and a two recirculation cells. Where, the right cell is bigger than the left one (plus one cell in the middle of the cavity). The open lines are pushed by the right recirculation cell. The isotherms of this case display that the planes S_1 and S_2 are more ventilated than the S_3 and S_4 ones. This demonstrates that the inclination is in favor of the left block cooling. By increasing Reynolds number to 300, $\varphi = 90^\circ$, we note that the solution is still an UCLF type as shown in *Fig.2j*. More, the left recirculation cell increases and mixes with the convective one. The isotherms of this case show that the left plane S_2 and the superior parts of the planes (S_1 and S_3) are well ventilated. The plane S_4 is badly ventilated. At $Re=500$, $\varphi = 90^\circ$, *Fig.2k*, we observe the appearance of a convective cell above the right block. The isotherm lines display that the plane S_2 is more ventilated than the plane S_4 . The lower parts of the planes (S_1 and S_3) are badly ventilated. At $Re=1000$, $\varphi = 90^\circ$, we notice that the solution has recovered its symmetry as displayed in *Fig.2l*; this solution is an ICF type. The open lines are all parallel to the axis passing through the openings. They flow between the convective cells and the two recirculation ones. The thermal fields of this case show that the upper parts of the planes (S_1 and S_3) are well ventilated. They show also that the plane S_2 is more ventilated than S_4 . Therefore, we can say that the Re

increasing helps the solution to get back its symmetry.

b. Case of $Ra=5.10^5$

By increasing the Rayleigh number to 5.10^5 , we remark the existence of a double solution: solution 1, *Fig.3a*, and solution 2, *Fig.3b*, for $Re=200$ and $\varphi=90^\circ$, these solutions are multi cellular. Because, after the convergence of the program, it appears an air bubble as shown in *Fig.4*.

The flow structure of solution 1, *Fig.3a*, is composed of one convective cell above the left block and two recirculation cells. The right recirculation cell increases and arrives to the upper part of the cavity. The isothermal lines display that the planes S_2 and S_3 are well ventilated, or, the other planes are badly ventilated and the air jet is very close to the right vertical plane. However, the flow structure of solution 2, *Fig.3b*, is different to that of solution 1; it is made up of two convective cells and two recirculation ones. The left recirculation cell increases and fills the left superior part of the micro-cavity. The thermal fields of this case illustrate that the lower parts of the heated vertical planes S_1 and S_3 are badly ventilated. They illustrate also that the left horizontal plane is more ventilated than the right horizontal one. The major part of the air jet is straight and parallel to the symmetry axis.

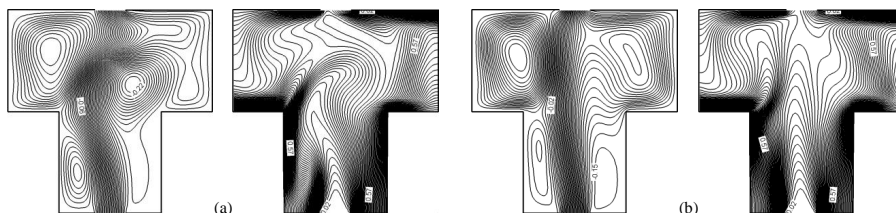


Figure 3: Streamlines and isotherms of solutions (solution 1: (a) and solution 2: (b)) for $Re=200$ and $\varphi=90^\circ$.

c. Case of $Ra=10^6$

Increasing Rayleigh number up to 10^6 leads to streamlines, similar to those obtained for $Ra=10^5$ with an intensification of the convective cells and the forced flow dominates on the natural convection (the forced flow is well installed). More, we note the existence of a multi-cellular solution. In this case, the flow structure is also symmetric for all cases without inclination ($\varphi=0^\circ$). Where at $Re=100$, *Fig.2a*, obtained by Najam and al (2003), we notice that the solution is an ICF type and the flow symmetry is conserved. The flow field is composed of open lines, two recirculation cells and two convective cells which fill the whole space of the upper part of

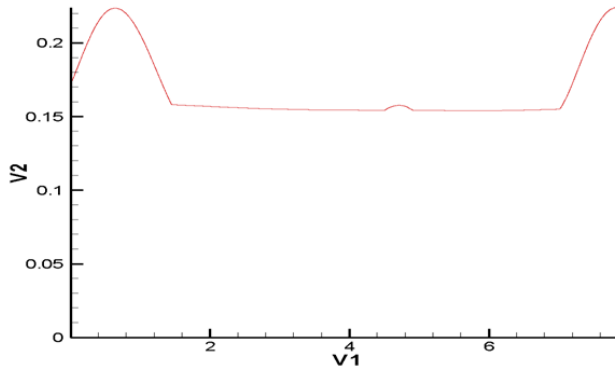


Figure 4: Convergence of the program for $Re=200$ and $\varphi = 90^\circ$.

the cavity where natural flow dominates on the forced convection. The isotherms of this case display that the fresh air fills the middle of the micro-cavity. The horizontal planes are more ventilated than the vertical ones. It is due to the rotation of the convective cells which take the cold from the upper wall to the horizontal planes of the two blocks. However, at $Re=1000$, $\varphi = 0^\circ$, we notice that the solution (ICF) is multi-cellular and symmetric as displayed in *Fig.5b*. This figure shows the appearance of four recirculation cells and other new cells. The intensity of the convective cells is reduced by the air jet. Furthermore, the open lines take the majority of the cavity and the forced flow is installed. The isotherms display a well cooling of all the planes which is due to the increase of Re . The fresh air fills the entire cavity.

By inclining the cavity, $Re=200$, $\varphi = 36^\circ$, *Fig.5c*, we remark that the solution becomes asymmetric, it is an UCLF type. The flow structure is made up of a convective cell above the plane S_2 , one small cell above the right block, one recirculation cell in the upper part of the micro-cavity and open lines which are deformed by the left convective cell. The thermal fields of this case show that there is an important ventilation of the planes S_1 , S_2 and S_3 . The right part of the upper wall is well ventilated. In addition, the fresh air fills the micro-cavity and it gets closer to the right vertical plane because of the important temperature gradient near this plane.

The increasing of Re to 300, $\varphi = 36^\circ$, leads to the decreasing of the left convective cell as illustrated in *Fig.5d*. More, the plane S_4 starts to exchange very well the heat with the air jet. At $Re=500$, $\varphi = 36^\circ$, *Fig.5e*, we note that the symmetry is destroyed and the solution is still an UCLF type. Where, the left convective cell size is reduced by the air jet intensity. The open lines are divided into two parts and turn around the convective cell. Two recirculation cells appear in the lower part of the micro-cavity. The isothermal lines of this case display that all the planes are well

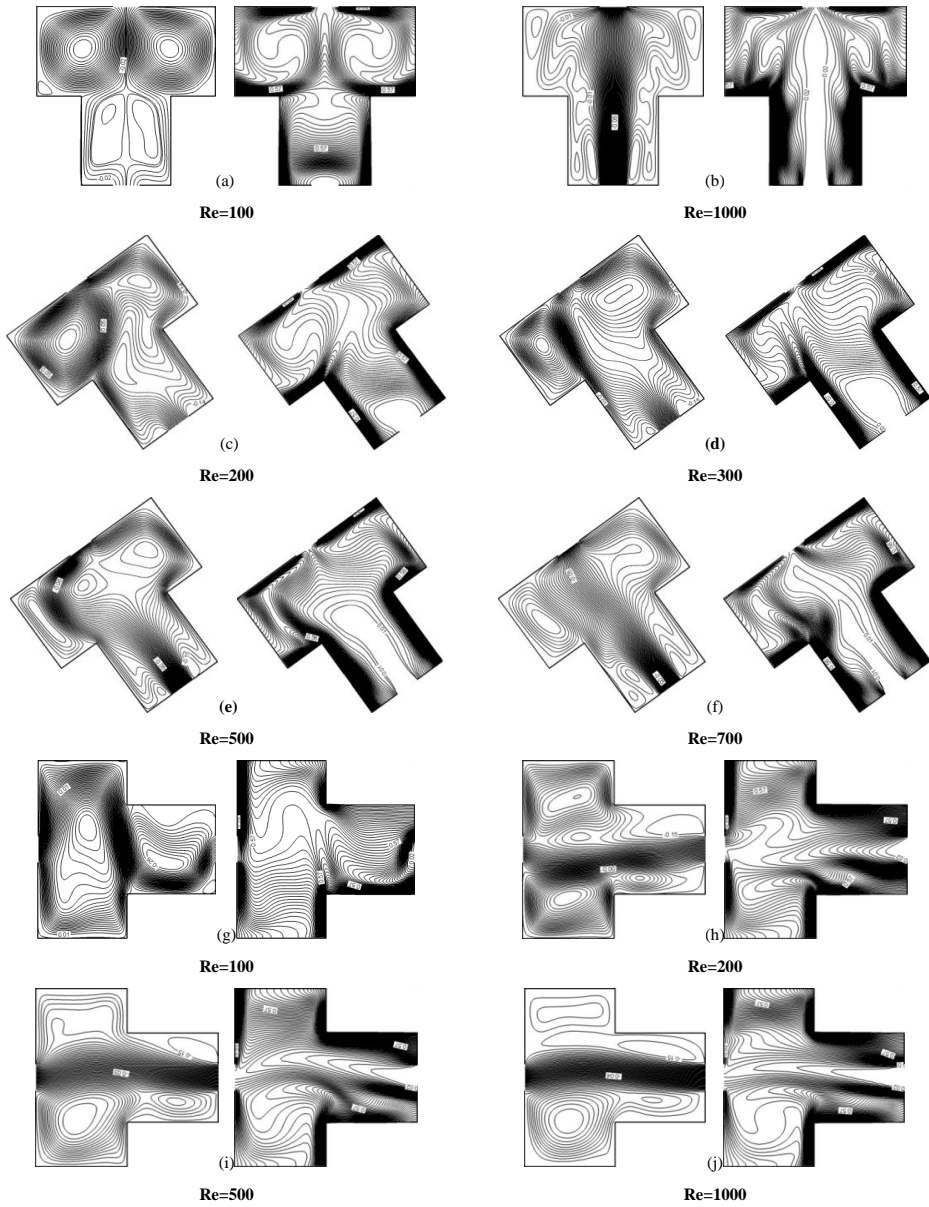


Figure 5: Streamlines and isotherms for $Ra=10^6$ and for different values of φ ; $\varphi=0^\circ$: {(a),(b)}; $\varphi=36^\circ$: {(c),(d),(e),(f)}; $\varphi=90^\circ$: {(g),(h),(i),(j)}.

ventilated. The flow shows that the air jet arrives to the upper part of the cavity. In addition, for high values of Reynolds number, $Re=700$, $\varphi = 36^\circ$, *Fig.5f*, we remark the same phenomenon as the previous case ($Re=500$), where the left convective cell size is increased. The open lines are divided into two parts, one part is parallel to the symmetry axis and the other one turns around the right Rayleigh-Bénard cell. The thermal fields of this case display that all the blocks are well cooled. They show also that the increase of Re improve the ventilation of the plane S_4 .

By increasing the inclination angle, $Re=100$, $\varphi = 90^\circ$, *Fig.5g*, we notice that the symmetry of the solution (UCLF) is not conserved. The flow structure is made up of open lines which are pushed by a large convective cell, where, the Rayleigh-Bénard convection is intense above the left block. The recirculation cell lies in almost the entire micro-cavity. The isotherms of this case display that the left block is more ventilated than the other one. They display also that the air jet is very close to the right vertical plane. At $Re=200$, $\varphi = 90^\circ$, *Fig.5h* shows that there exists two recirculation cells and a small one between two convective cells. The right convective cell increases and the left one lies inside the micro-cavity. The corresponding isothermal lines of this case demonstrate that the plane S_2 is more ventilated than the plane S_4 . In spite of increasing Reynolds number to 500, *Fig.5i*, we observe that the solution is still asymmetric (UCLF). The right convective cell has disappeared and the majority of the open lines are deformed by the left convective cell. The isotherms of this case show the well ventilation of the planes S_2 and S_3 . The vertical walls are badly ventilated. However, for $Re=1000$, $\varphi = 90^\circ$, we remark that the solution starts to recover its symmetry and becomes an ICF type as displayed in *Fig.5j*. A convective cell appears above the right block. The left recirculation cell lies in the superior part of the cavity, because of the convective ones effect and so all the open lines are parallel to the symmetry axis. The isotherms of this case display that the lower parts of the planes S_1 and S_3 are badly ventilated while the plane S_2 is more ventilated than the plane S_4 . They display also that the increase of Re improve the ventilation of the plane S_4 .

3.2 Heat transfer:

The local Nusselt numbers Nu_L and Nu_R variations with Re and φ are presented in figures : *Fig.6,7,8,9,10* for different values of Reynolds number $100 \leq Re \leq 1000$ and inclination angle $0^\circ \leq \varphi \leq 90^\circ$ ($Ra=10^5$ and $Ra=10^6$).

a. Case of $Ra=10^5$

We notice generally, that Nu_L decreases with Re till a minimum, then it increases. More, we note that in the forced convection ($500 \leq Re \leq 1000$) zone, the heat transfer is similar for different values of the inclination angle in the left block. In the other

hand, we remark that Nu_R increases with Re till a maximum, then decreases, and then it increases. *Fig.6* shows that by increasing the inclination angle φ , Nu_R decreases for Re between 100 and 300, where, the natural convection dominates on the forced flow. For Re between 300 and 500, we note that there is a competition between forced and natural flow. Or, for high values of Re , we notice that the Nu_R curves are similar for different values of the inclination angle.

However, we observe that for the low values of Re , Nu_L presents a maximum with φ , which moves to the right, when Re varies from 100 to 500 as illustrated in *Fig.7*. Or, for $Re=700$, the Nu_L curve becomes monotonic increasing. Instead, Nu_R begins to decrease insteadily with φ ($Re=100$) where a maximum of Nu_R with φ begins to be felt. This maximum moves to the lower inclinations (to the left), when Re varies from 200 to 700.

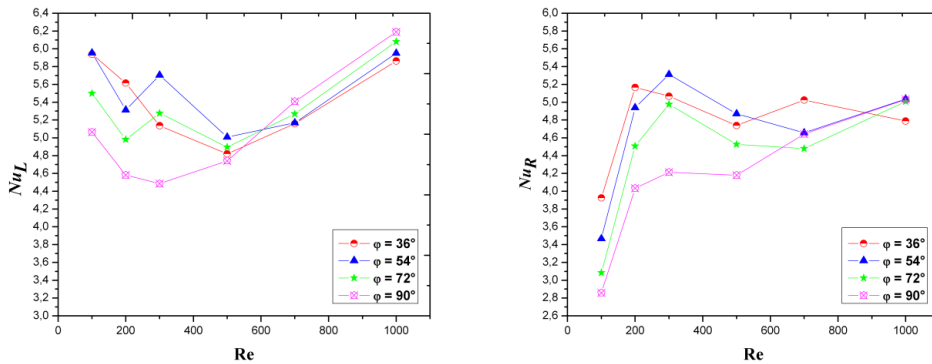


Figure 6: Nu_L and Nu_R variations with Re for $Ra=10^5$ and different values of φ .

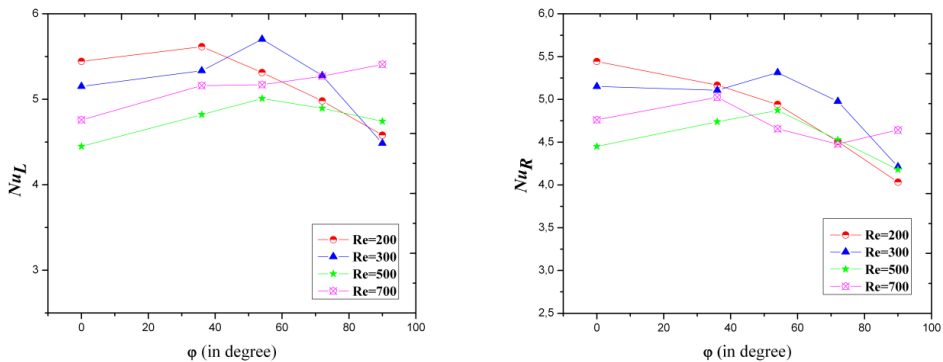


Figure 7: Nu_L and Nu_R variations with φ for $Ra=10^5$ and different values of Re .

b. Case of $Ra=10^6$

In this case, we notice that Nu_L varies irregularly with Re while Nu_R varies in the same way with Re for all inclination angles $36^\circ \leq \varphi \leq 90^\circ$ as displayed in Fig.8. This means that the heat transfer, between the left block and the air jet, is similar for all inclination angles. We remark also that the increase of φ leads to the decrease of Nu_L and Nu_R . For that, by increasing φ , the heat transfer decreases for the two blocks.

On the other hand, we notice that Nu_L increases with the inclination angle φ , then, it decreases in the zone where the mixed convection is installed ($300 \leq Re \leq 500$) as shown in Fig.9. While, in the zone where the forced convection dominates ($Re=1000$), we note that Nu_L is steady (stable) between 0° and 72° , then, it increases slowly. The heat transfer between the left block and the air jet is weak ($Re=1000$). Nevertheless, for the variation of Nu_R with φ , we observe that Nu_R decreases with φ then, it varies in the same way for $300 \leq Re \leq 1000$. Besides, the heat transfer between the right block and the imposed air jet ($Re=1000$) is lower.

Nonetheless, we observe that Nu_g varies in the same way with Re in the mixed convective zone ($100 \leq Re \leq 500$) for the lower inclinations $36^\circ \leq \varphi \leq 54^\circ$ as illustrated in Fig.10, then it decreases with Re . But for $\varphi=90^\circ$, we remark that Nu_g increases slowly with Re . Moreover, we notice that the increase of φ leads to the decrease of Nu_g . Hence, by increasing φ , the heat exchange through the cavity decreases (between the air jet and the two blocks).

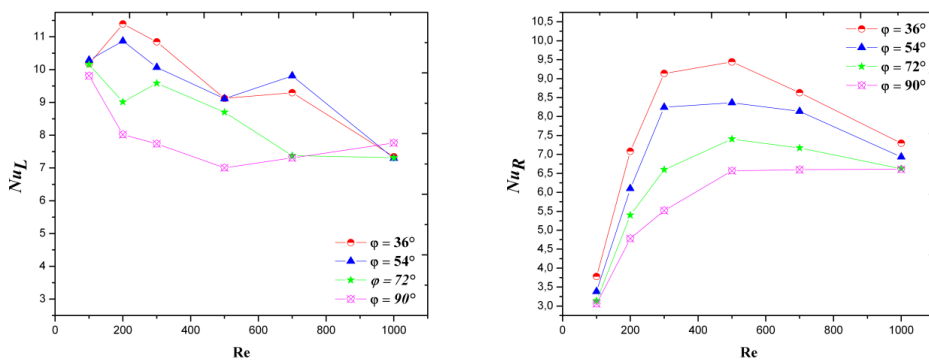


Figure 8: Nu_L and Nu_R variations with Re for $Ra=10^6$ and different values of φ .

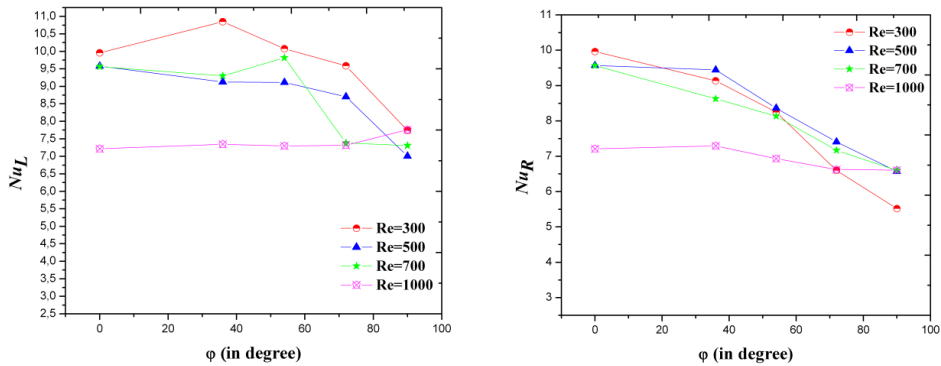


Figure 9: Nu_L and Nu_R variations with ϕ for $Ra=10^6$ and different values of Re .

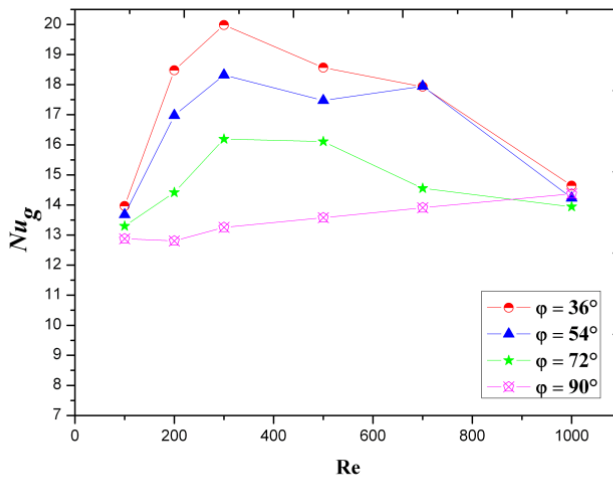


Figure 10: Nu_g variations with Re for $Ra=10^6$ and different values of ϕ .

4 Conclusion

We have studied numerically the mixed flows in inclined “ T ” form cavity. The emphasis is given to the effect of the inclination angle on the flow structure and heat transfer.

Among the results obtained, we have found two types of solution (ICF and UCLF) by varying Re and ϕ . By increasing Ra , the convective cells size increases while the recirculation cells size increases with Re . The inclination angle variation has a significant effect on the solution symmetry and the Re increasing helps the solution to recover its symmetry.

According to the results, the inclination is in favor of the ventilation of the left block. The heat transfer between the blocks and the forced air jet ($Re=1000$) is the smallest one. In the case of $Ra=10^5$, Nu_L and Nu_R decreases with φ for small Reynolds number. Also, in the case of $Ra=10^6$, the increase of φ leads to the decrease of Nu_L and Nu_R . In addition, the heat exchange through the whole cavity decreases by increasing the inclination angle ($Ra=10^6$).

Reference

Al-Ajmi, R.; Mosaad, M. (2012): Heat Exchange between Film Condensation and Porous Natural Convection across a Vertical Wall. *Fluid Dyn. Mater. Process*, vol. 8, no. 1, pp. 51-68.

Amahmid, A.; Hasnaoui, M.; Vasseur, P. (1997): Multiplicité des solutions en convection naturelle dans une géométrie répétitive. *Int. J. Heat Mass Transfer*, vol. 41, no. 16, pp. 3805-3818.

Arid, A.; Kousksou, T.; Jegadheeswaran, S.; Jamil, A.; Zeraouli, Y. (2012): Numerical Simulation of Ice Melting Near the Density Inversion Point under Periodic Thermal Boundary Conditions. *Fluid Dyn. Mater. Process*, vol. 8, no.3, pp. 257-276.

Bakkas, M.; Amahmid, A.; Hasnaoui, M. (2006): Steady natural convection in a horizontal channel containing heated rectangular blocks periodically mounted on its lower wall. *Energy Conversion and Management*, vol. 47, pp. 509-528.

Bejan, A.; Sciubba, E. (1992): The optimal spacing of parallel plates cooled by forced convection. *Int. J. Heat Mass Transfer*, vol. 35, no. 18, pp. 3259-3264.

Chen, Y.; Kang, S.; Tuh, W.; Hsiao, T. (2004): Experimental investigation of fluid and heat transfer in micro-channels. *Tamkang Journal of Science and Engineering*, vol. 7, no. 1, pp. 11-16.

Choukairy, K.; Bennacer, R. (2012): Numerical and Analytical Analysis of the Thermosolutal Convection in an Heterogeneous Porous Cavity. *Fluid Dyn. Mater. Process*, vol. 8, no.2, pp. 155-172.

Desrayaud, G.; Fichera, A. (2002): laminar natural convection in a vertical isothermal channel with symmetric surface mounted rectangular ribs. *Int. J. Heat and Fluid Flow*, vol.23, pp. 519-529.

Dihmani, N.; Amraoui, S.; Mezrhab, A.; Laraqi, N. (2012): Numerical Modelling of Rib Width and Surface Radiation Effect on Natural Convection in a Vertical Vented and Divided Channel. *Fluid Dyn. Mater. Process*, vol. 8, no.3, pp. 311-322.

El Alami, M.; Semma, E. A.; Oubarra, A.; Penot, F. (2004): Chimney effect in a

“ T ” form cavity with heated isothermal blocks: The blocks height effect. *Energy Conversion and Management*, vol. 45, pp. 3181-3191.

El Alami, M.; Semma, E. A.; Boutarfa, R. (2009): Numerical Study of Convective Heat Transfer in a Horizontal channel. *FDMP*, vol. 5, no. 1, pp. 23-36.

El Alami, M. (2005): Etude numérique de la convection naturelle dans un canal muni d'ouvertures et de blocs chauffants, Thèse de doctorat.

Hamimid, S.; Guellal, M.; Amroune, A.; Zeraibi, N. (2012): Effect of a Porous Layer on the Flow Structure and Heat Transfer in a Square Cavity. *Fluid Dyn. Mater. Process*, vol. 8, no. 1, pp. 69-90.

Haslavsky, V.; Miroshnichenko, E.; Kit, E.; Gelfgat, A. Yu. (2013): Comparison and a Possible Source of Disagreement between Experimental and Numerical Results in a Czochralski Model. *Fluid Dyn. Mater. Process*, vol. 9, no. 3, pp. 209-234.

Kalache (1987): Contribution à l'étude de la convection naturelle en cavités trapézoïdales chauffées par dessous. Thèse de l'Université de Poitiers.

Kamath, P. M.; Balaji, C.; Venkateshan, S. P. (2013): Heat transfer studies in a vertical channel filled with porous medium. *Fluid Dyn. Mater. Process*, vol. 9, no. 2, pp. 109-124.

Lappa, M. (2013): On the Existence and Multiplicity of One-dimensional Solid Particle Attractors in Time-dependent Rayleigh-Bénard Convection. *Chaos*, vol. 23, pp. 013105 (9 pages).

Lappa, M. (2011): Some considerations about the symmetry and evolution of chaotic Rayleigh-Bénard convection: The flywheel mechanism and the “wind” of turbulence”. *Comptes Rendus Mécanique*, vol. 339, pp. 563-572.

Leonart, B. P. (1979): A stable and accurate convective modeling procedure.

Mahmoudi, A.; Mejri, I.; Abbassi, M. A.; Omri, A. (2013): Numerical Study of Natural Convection in an Inclined Triangular Cavity for Different Thermal Boundary Conditions: Application of the Lattice Boltzmann Method. *Fluid Dyn. Mater. Process*, vol. 9, no. 4, pp. 353-388.

Mahrouche, O.; Najam, M.; El Alami, M.; Faraji, M. (2013): Mixed Convection Investigation in an Opened Partitioned Heated Cavity. *Fluid Dyn. Mater. Process*, vol. 9, no. 3, pp. 235-250.

Maougah, A.; Bessaïh, R. (2013): Heat Transfer and Entropy Analysis for Mixed Convection in Discretely Heated Porous Square Cavity. *Fluid Dyn. Mater. Process*, vol. 9, no. 1, pp. 35-58.

Meskini, A.; Najam, M.; El Alami, M. (2011): Convective mixed heat transfer in a square cavity with heated rectangular blocks and submitted to a vertical forced

flow. *FDMP*, vol. 7, no. 1, pp. 97-110.

Moufekkir, F.; Moussaoui, M. A.; Mezrhab, A.; Naji, H.; Bouzidi, M. (2012): Numerical Study of Double Diffusive Convection in presence of Radiating Gas in a Square Cavity. *Fluid Dyn. Mater. Process*, vol. 8, no. 2, pp. 129-154.

Najam, M.; El Alami, M.; Hasnaoui, M.; Amahmid, A. (2003): Convection mixte dans une cavité en forme de “T”, munie de blocs chauffants: Effet de la hauteur des blocs. *Phys. Chem. News*, vol. 9, pp. 50-57.

Najam, M.; El Alami, M.; Oubarra, A. (2004): Heat transfer in a “ T ” form cavity with heated rectangular blocks submitted to a vertical jet: the block gap effect on multiple solutions. *Energy Conversion and Management*, vol. 45, pp. 113-125.

Najam, M.; Amahmid, A.; Hasnaoui, M.; El Alami, M. (2003): Unsteady mixed convection in a horizontal channel with rectangular blocks periodically distributed on its lower wall. *International Journal of Heat and Fluid Flow*, vol. 24, pp. 726-735.

Patankar, S. V. (1980): *Numerical heat transfer and fluid flow*. Hemisphere Publishing Corporation. Washington D.C.

Rana, G. C.; Thakur, R. C. (2013): Effect of Suspended Particles on the Onset of Thermal Convection in Compressible Viscoelastic Fluid in a Darcy-Brinkman Porous Medium. *Fluid Dyn. Mater. Process*, vol. 9, no. 3, pp. 251-266.

Rouijaa, H.; El Alami, M.; Semma, E. A.; Najam, M. (2011): Natural convection in a inclined T-Shaped Cavity. *FDMP*, vol. 7, no. 1, pp. 57-70.

Sharma, C.; Zimmermann, S.; Tiwari, M.; Michel, B.; Poulikakos, D. (2012): Optimal thermal operation of liquid-cooled electronic chips. *Int. J. Heat Mass Transfer*, vol. 55, pp. 1957-1969.

Young, T. J.; Vafai, K. (1998): Convective cooling of heated obstacle in a channel. *Int. J. Heat Mass Transfer*, vol. 41, pp. 3131-3148.

Young, T. J.; Vafai, K. (1998): Convective flow and heat transfer in a channel containing multiple heated obstacles. *Int. J. Heat Mass Transfer*, vol. 41, pp. 3279-3298.

Zeng, Y.; Vafai, K. (2009): An investigation of convective cooling of an array of channel-mounted obstacles. *Numerical Heat Transfer, Part A*, vol. 55, pp. 967-982.

